

High Energy Phenomena In The Universe

Arnon Dar¹

ABSTRACT

Highlights of the 44th Rencontre De Moriond on High Energy Phenomena In The Universe which was held in La Thuile, Italy during February 1-8, 2009.

1. Introduction

More than 110 talks and 10 posters were presented at the 44th Rencontre De Moriond on high energy phenomena in the universe. They reflect the flood of new and important results in the fields of cosmic ray astrophysics, high energy gamma ray astronomy, high energy neutrino astronomy and the search for astrophysical evidence of physics beyond the standard models of particle physics, general relativity and cosmology. Unable to cover in a short summary all the talks and the new results, I will limit my summary and comments to results which were presented and discussed in this Rencontre and which to the best of my judgment are the most important and fundamental ones.

2. Ultra-high Energy Cosmic Rays

If the ultra-high energy cosmic rays (UHECRs) observed reaching Earth are extragalactic in origin, as suggested by the isotropy of their arrival directions and the lack of correlation with the Galactic plane, than inelastic collisions with the cosmic background radiation (CBR) and cosmic expansion are expected to degrade their energies during their travel from their extragalactic sources to Earth. If the UHECRs are protons, pion production in collisions with the cosmic microwave background radiation (MBR) strongly degrades their energy above an effective threshold of $\sim 5 \times 10^{19}$ eV, the so called Greisen-Zatsepin-Kuzmin (GZK) threshold (1),(2) while e^+e^- pair production in collisions with the CBR degrades their energy above an effective threshold of $\sim 10^{18}$ eV just below the CR ankle at $\sim 3 \times 10^{18}$ eV. If the UHECRs are nuclei, nuclear photodissociation in collisions with the CBR begins

¹arnon@physics.technion.ac.il

Physics Department, Technion, Haifa 32000, Israel

to be effective at a slightly lower energy for light nuclei and around the GZK threshold energy for iron-like nuclei (3). Thus, the suppression of the flux of CR protons above the GZK threshold is expected to be accompanied by even a stronger suppression of the flux of heavier nuclei.

Early measurements by the Akeno Giant Air Shower Array (AGASA), which detects air showers at ground level with scintillators, reported the detection of UHECRs above the GZK threshold not showing the expected GZK suppression (4) but showing strong clustering in their arrival direction. These led to variety of interpretations including speculations on physics beyond the standard particle physics model and on violation of Lorentz invariance and special relativity. However, later results from the High Resolution Fly’s Eye (HiRes) experiment (5),(6), which detect the fluorescence emitted in the air by nitrogen molecules excited by the passage of the shower, observed the GZK suppression above the expected threshold and did not find a significant unisotropy in the arrival directions of UHECRs. The AGASA and HiRes results were based on a small number of events and used different techniques. Results from measurements of UHECRs by the Pierre Auger Observatory which was conceived as a hybrid detector combining the two detection methods and covering an area 30 times bigger than that of AGASA, that were obtained during its construction confirmed the GZK suppression above the expected threshold (7),(8) and appeared to indicate that UHECRs above the GZK threshold arrive from nearby active galactic nuclei (9),(10).

The fast falling spectrum of the ultra-high energy cosmic rays (UHECRs), up to energies of about 10^{20} eV where the CR flux is of the order of 1 particle per km^2 per a couple of centuries, their arrival directions and their composition have now been measured by HiRes (6) and by the PAO (8),(11),(12) with sizable statistics (roughly twice and four times, respectively, the exposure of AGASA). The main results can be summarized as follows:

- **GZK Suppression Confirmed:** Allowing for 10% adjustment in the CR energies inferred either by HiRes or PAO from the fluorescence light emitted by air molecules excited by the CR induced atmospheric showers, because of a 10% difference in the adopted fluorescence yield in the showers, the energy spectra of UHECRs measured by both experiments are identical (Fig. 1a) and show the expected GZK suppression beyond $\sim 4 \times 10^{19}$ eV, consistent with the highest energy CRs being extragalactic protons. (The power law $E^{-2.69}$ which fits the PAO spectrum below 40 EeV predicted 163 ± 3 events above 40 EeV and 35 ± 1 above 100 EeV, while 69 events and 1 event were observed by PAO, clearly confirming the GZK suppression).
- **Composition:** The atmospheric depth (in g/cm^2) of shower maximum, X_{max} , has been used both by HiRes (6) and PAO (11),(13) to infer the composition of UHECRs.

Both experiments report a mixed composition that is becoming lighter with energy up to 3 EeV. However, HiRes results indicate a light composition all the way up to the GZK threshold around 40 EeV where it runs out of statistics, whereas PAO results indicate that the composition becomes heavier above 3 EeV and more so beyond the GZK threshold (Fig. 1b). These conclusions are valid provided that hadron physics does not change above 3 EeV.

- **Isotropy:** Below the GZK threshold both the HiRes and the PAO CR events are completely consistent with statistical fluctuations of an isotropic distribution of arrival directions.
- **UHECRs-AGN correlation:** At energies above the GZK threshold only CRs from nearby sources can reach Earth. If they are not deflected much by the intergalactic and Galactic magnetic fields, their arrival directions should point back to their sources, opening the window to UHECR astronomy. The evolution with energy of the distribution of arrival directions of UHECRs measured by PAO shows a sharp transition from isotropy to anisotropy beyond the GZK threshold. The arrival directions of UHECRs with energy above 57 EeV show a correlation on angular scales of less than 6° with the sky positions of AGNs within 71 Mpc, which are concentrated near the supergalactic plane. Intrinsic (catalog independent) properties of these events, such as their auto-correlation function, show a clear departure from isotropy in a large angular range (12). The correlation/unisotropy observed by PAO was not confirmed by HiRes which reported (6) lack of arrival-direction correlation of their highest energy events with local AGNs (in the Northern Hemisphere). PAO found that out of their 27 UHECRs events with energy above 56 EeV, 20 were found to lie within 3.2° of the line of sight to an AGN nearer than 71 Mpc (Fig. 2a) while only 6 were expected to be found by chance from an isotropic distribution of arrival directions (the threshold energy, maximal angular deviation, and maximal AGN distance were chosen to maximize the UHECRs-correlation). HiRes found that using the PAO criteria only 2 of their 13 events above 56 EeV correlated with AGN (Fig. 2b), while 3.2 were expected randomly, ruling out the correlation at a probability of 83%. The PAO collaboration has stressed that even though the correlation with nearby AGN seems to be quite robust in their sample, the angular scale of $\sim 6^\circ$ does not make possible to unambiguously identify the sources and sources which are distributed similar to AGNs cannot be excluded as the true sources.
- **UHEGRs:** Showers initiated by ultra-high energy gamma rays (UHEGRs) develop differently from showers induced by nuclear primaries. Particularly, the depth of shower maximum is much larger and the shower is much poorer in muons relative to those

of CR nuclei. Upper limits on the presence of photons in the primary cosmic-ray flux were obtained by PAO; in particular a limit of 2% (at 95% c.l.) above 10 EeV on the flux of UHEGRs relative to UHECRs was derived by PAO (13). This limit improves previous constraints on Lorentz violation parameters by several orders of magnitude due to the extreme energy in case of UHEGRs.

Although AGN are a natural source of extragalactic UHECRs, the directional correlation found by Auger is surprising in many respects. A 3.2° deviation is of the order of magnitude of that inflicted on UHECRs by the magnetic field of the Galaxy, it would be surprising if extragalactic CRs did not encounter intergalactic magnetic fields with similar or larger effects. The Veron catalog of AGN is not complete and not directionally uniform in its coverage and sensitivity, unlike the Auger coverage within its field of view. The Auger correlation is purely directional, not investigated case-by-case for the possible effects of AGN distance, luminosity, jet direction and radio loudness. The effect of distance is obvious, the correlation with luminosity is very plausible. Concerning jet-direction, one has to understand how the UHECRs from AGNs could be fairly isotropically emitted, given that AGNs produce extremely collimated jets, and that they are seen in gamma-rays as very luminous blazars only when the jets are pointing in our direction. The proton- and electron-acceleration efficiencies of CR sources are presumably correlated. The radio loudness is a measure of the number of high energy synchrotron-radiating electrons. The jets of an AGN may accelerate CRs to well above the GZK limit and collimate them forward in a cone of aperture $1/\Gamma$ where Γ is their bulk motion Lorentz factor. But the PAO results suggest a more isotropic source, the end lobe of an AGN jet being the obvious choice (14). These lobes have radii R_l of a few kpc. They are steadily energized by the incoming jet. Traveling in a medium swept up by previous jet components, a jet may deposit in its lobe an energy in excess of 10^{60} erg, emitted by the central black hole during the AGNs active life. An equipartition magnetic field B in these end lobes can exceed a milli Gauss. The Larmor limit energy for the acceleration of a proton in a lobe is then $E_{max} \approx e B R_L \approx 3 \times 10^{21}$ eV, well above the GZK threshold.

However, the PAO UHECRs-AGN correlation is puzzling in other respects. E.g., why there are no events from the direction of the Virgo cluster, that contains powerful AGN such as M87 at 14 Mpc? Why the maximal correlation for UHECRs with $E \geq 57$ EeV is with AGN at distance less than 71 Mpc - Such UHECRs should come from distances up to 200 Mpc and not only from less than 71 Mpc.

All together, the results from PAO are very important in many respects and are pointing towards a potential breakthrough in UHECR and UHEGR astronomies, but much more statistics are needed in order to establish that. With a main goal of full sky coverage, the

Auger Observatory is to be completed by a northern site. Current plans aim at a significantly ~ 7 times larger array to proceed with UHECR and UHEGR astronomies.

To reach even larger exposures, dedicated observatories in space which can observe UHECR induced atmospheric showers by looking down towards the Earth are planned. The Extreme Universe Space Observatory (EUSO) on the Japanese Experiment Module (JEM), which will detect fluorescence from UHECR events within 60° field of view, is being planned for deployment on the International Space Station. JEM-EUSO may detect $\sim 1,000$ particles above 70 EeV in a three year mission. The Orbiting Wide-Angle Light Collectors (OWL) will stereoscopically image fluorescence from UHECRs. Such missions may observe a significant fraction of the ~ 10 million showers generated in the Earth atmosphere per year by UHECRs with energy above the GZK threshold.

3. Dark Matter

3.1. Evidence from cosmic colliders

Dark matter is an hypothetical matter that does not emit electromagnetic radiation, whose presence has been inferred consistently from gravitational effects on visible matter, on light trajectories, on the space-time geometry of the universe, on structure formation in the universe and on cosmic evolution.

The observed phenomena which imply that the universe contains much more dark matter than visible matter, include the rotational speeds of galaxies, orbital velocities of galaxies in clusters, gravitational lensing of background objects by galaxies and galaxy clusters and the temperature distribution of hot gas in galaxies and clusters of galaxies. Dark matter also plays a central role in structure formation and galaxy evolution, and has measurable effects on the anisotropy of the cosmic microwave background radiation. At present, the density of ordinary baryons and radiation in the universe is estimated about 4% of the total energy density in the universe. About 22% is thought to be composed of dark matter. The remaining 74% is thought to consist of dark energy, distributed diffusely in space.

The dark matter hypothesis has generally been the preferred solution to the missing mass problems in astronomy and cosmology over alternative theories of gravity based on modifications to general relativity which have been used to model dark matter observations without invoking dark matter (15),(16). However, until recently there was no conclusive evidence that dark matter really exists. This has changed dramatically by X-ray and optical observations of collisions between galaxy clusters (17),(18),(19), such as in 1E0657-558 at $z=0.296$ (the ‘Bullet Cluster’), MACS J0025 at $z=0.586$ and A520 at $z=0.201$ (the ‘Cosmic

Train Wreck’). In such collisions the clusters’ galaxies and dark matter halos are affected only by gravity while the electromagnetic interactions between the clusters’ X-ray emitting ionized gas produce an additional drag on the gas. Consequently, after the collision the galaxies and their associated dark matter halos lead the slower moving X-ray emitting gas clouds stripped off from the galaxy clusters, as seen in Figs. 3a,3b. The galaxies in these Figures were observed from the ground with Magellan and from space with the HST, the stripped off X-ray emitting gas was mapped with Chandra and the dark matter halos of the clusters were mapped by measuring the distortion of the images of background galaxies by the deflection of light as it passes the clusters dark matter halos. Such observations require that regardless of the form of the gravitational force law at large distances and low accelerations, the majority of the mass of the system be some form of dark matter. Many more cases of cluster collisions will be studied through gravitational lensing of background galaxies with a dedicated large telescope such as the 8.4m Large Synoptic Survey Telescope (LSST) which is under design and development and scheduled to be commissioned at Cerro Pachn (Chile) by 2017 (17).

3.2. Direct and indirect detections ?

Determining the nature of the dark matter particles is one of the most important problems in modern cosmology and particle physics. Both direct detection in which the interaction of dark matter particles are observed in a detector and indirect detection that looks for the products of dark matter annihilation or decay products have been conducted extensively and are ongoing. Dark matter detection experiments have ruled out some WIMP (Weakly Interacting Massive Particle) and axion models. There are also several claims of direct detection of dark matter particles in lab experiments such as DAMA/NaI (Dark Matter/Sodium Iodine) in the Gran Sasso underground laboratory, and possible detections of astrophysical gamma rays, positrons and electrons from dark matter annihilation, by EGRET aboard the CGRO, by ATIC and by PAMELA, respectively, but all these are so far unconfirmed and difficult to reconcile with the negative results of other experiments. In particular:

3.2.1. The EGRET GeV excess:

The spectrum of the diffuse γ background radiation (GBR) that was measured by EGRET aboard the Compton Gamma Ray Observatory showed an excess above 1 GeV in comparison with the flux expected from interactions of cosmic ray (CR) nuclei and electrons in the Galactic interstellar medium (ISM) (20). The origin of this GeV excess has been

unknown. Among its suggested origins was annihilation or decay of WIMPs (21). However, recent measurements with the Large Area Telescope (LAT) aboard the Fermi observatory have yielded preliminary results (22) which do not show a GeV excess at small Galactic latitudes and agree with the flux expected from CR interactions in the Galactic ISM (Fig. 4a). Also, the extragalactic GBR measured by EGRET does not show a corresponding ‘GeV excess’ (Fig. 4b). which would be expected from such dark matter annihilation/decay in external galaxies and in the IGM. Moreover, by comparing the spectra of gamma-rays around one GeV from nearby Galactic pulsars, which were measured by EGRET and LAT, the Fermi collaboration confirmed (22) previous conclusions (23) that the origin of the EGRET GeV excess is probably instrumental and not a dark matter annihilation/decay signal.

3.2.2. The ATIC excess:

The Advanced Thin Ionization Calorimeter (ATIC) experiment aboard balloon flights over Antarctica (24) reported an excess in the flux of CR electrons at energies between 300-800 GeV. Several papers suggested that this excess in cosmic ray electrons (and positrons) arises from annihilation of dark matter particles such as Kaluza-Klein particles with a mass of about $620 \text{ GeV}/c^2$ (25)). However, in this meeting caution was advocated when interpreting cosmic ray electron and positron data above a few GeV because of possible proton contamination of the measurements and it was pointed out that the ATIC reported data should be suspected as the authors did not properly take into account the uncertainties associated with a potential hadronic background due to particle interactions inside the graphite target on top of the detector (26).

Moreover, it was pointed out (27) that if the ATIC electron excess was due to dark matter annihilation, such an excess of Galactic cosmic ray electrons would have produced a detectable GeV excess in the diffuse Galactic GBR at large latitudes, while dark matter annihilation in external galaxies would have produced a detectable GeV excess in the diffuse extragalactic GBR at all latitudes, which was not observed by EGRET (Figs. 5a,b).

After the Rencontre de Moriond it was shown that the ATIC excess is probably instrumental due to misidentified proton induced electron-like events in the ATIC detector by cosmic ray protons (29). Moreover, the HESS collaboration reported a measurement of the cosmic-ray electron spectrum above 340 GeV which does not show the ATIC peak (30) and the LAT collaboration reported a high precision measurement of the steeply falling cosmic ray electron spectrum between 20 GeV and 1 TeV which also does not show the prominent ATIC peak (31). The spectral index of the CR electrons (plus positrons) with energy

below 1 TeV which was measured by HESS and by PAMELA is consistent with -3.2 . This index is suggested by the spectral index 2.1 ± 0.03 of both the Galactic GBR at large latitudes and the extragalactic GBR (at all latitudes), which were measured by EGRET. However a significantly different spectral index -3.04 was measured by LAT. Additional measurements by LAT and by other experiments in space such as PAMELA, and in particular experiments with magnetic spectrometers such as AMS in space and on high altitude balloon experiments above the south pole, are highly desirable.

3.2.3. The PAMELA positron fraction:

In the standard leaky box models, CR sources accelerate primary cosmic ray nuclei and electrons while secondary electrons and positrons are produced by the decay of charged π 's and K 's produced in hadronic collisions of primary cosmic ray nuclei in the interstellar medium (ISM). The primary particles are injected with roughly the same energy spectrum $dn/dE \sim E^{-p_{inj}}$ with $p_{inj} \approx 2.2$, but the escape by diffusion from the Galaxy increases the spectral index of the primary CR nuclei to $p_N \approx 2.7$ while cooling by synchrotron radiation and inverse Compton scattering of background photons increases the spectral index of the primary CR electrons by one unit to $p_e \approx 3.2$. Because of Feynman scaling the secondary electrons and positrons, which are produced by CR interactions in the ISM, have a spectral index $p_{inj} \approx 2.7$, which increases to $p_e \sim 3.7$ by cooling. Consequently, in the standard CR model the positron fraction decreases like $\sim E^{-0.5}$ at high energies (where solar modulation and geomagnetic effects are negligible). Contrary to this expectation the PAMELA satellite experiment has recently reported (32),(33),(34), a dramatic rise in the positron fraction starting at 10 GeV and extending up to 100 GeV in complete disagreement with the standard cosmic ray model calculations (35). These observations have created much excitement and motivated many papers claiming that the observed rise is produced by the annihilation of dark matter particles. Other publications related the excess to a local enhancement of the flux of electrons and positrons due to nearby galactic sources of positrons and electrons such as pulsars (36) or to secondary production in the ISM by CRs from nearby sources such as supernova remnants in the nearest spiral arm (37).

However, the rise of the positron fraction with increasing energy beyond 10 GeV may be entirely due to hadronic production of positrons (and electrons) in the cosmic ray sources (27): In fact, if Fermi acceleration of highly relativistic particles results in a universal power-law distribution of Lorentz factors of the accelerated particles, $dn/d\gamma \propto \gamma^{-p_{inj}}$, with an injection spectral index $p_{inj} \approx 2.2$, than the injected flux of high energy electrons is suppressed by

a factor $(m_e/m_p)^{p_{inj}-1} \approx 10^{-4}$ compared to that of protons at the same energy (38), which is much smaller than their observed ratio in the Galaxy. Cosmic ray nuclei, however, may encounter in/near source a total column density comparable to a mean free path for hadronic interactions during their acceleration and before being injected into the ISM. In that case, due to Feynman scaling, they generate an electron+positron spectrum identical to that of the CR protons but with a normalization which is larger by roughly two orders of magnitude than that of the primary Fermi accelerated electrons. The combination of Fermi acceleration of electrons and hadronic production of electrons and positrons in/near the CR sources plus hadronic production of electrons and positrons in the ISM can naturally explain the rise of the positron fraction beyond 10 GeV (27).

Finally, despite of the above, caution must be applied also to the PAMELA results as emphasized in this Rencontre by M. Schubnell (26): The intensity of cosmic-ray protons at 10 GeV exceeds that of positrons by a factor of about 5×10^4 . Therefore a proton rejection of about 10^6 is required if one wants to obtain a positron sample with less than 5%. Furthermore, because the proton spectrum is much harder than the electron and positron spectra, the proton rejection has to improve with energy. In addition, any small amount of spillover from tails in lower energy bins can become problematic (26). Fig. 6a demonstrates that a proton contamination of 3×10^{-4} can explain the PAMELA positron fraction.

3.2.4. The PAMELA antiproton to proton ratio:

The recent measurements of the antiproton to proton ratio measured by PAMELA (32),(33) agrees with that expected from secondary production in the ISM, but the measurements do not extend to high enough energy (see Fig. 6b) where the energy dependence can distinguish between secondary production in the CR sources which yields a constant ratio and secondary production in the ISM that yields a ratio which decreases like $E^{-0.5}$.

4. High Energy Gamma Ray Astronomy

The tremendous progress made in high energy gamma ray astronomy during the past two decades is due to many instruments with increasing sensitivity covering now the entire MeV-PeV energy range, as summarized in Fig. 7 borrowed from Aldo Morselli.

This progress has culminated with the successful completion and operation of the large imaging Cherenkov telescope systems, HESS, MAGIC and VERITAS and the launch of the Fermi Gamma-ray Space Observatory on June 11, 2008 with its two main instruments, the

Large Area Telescope (LAT) for all-sky survey studies of astrophysical and cosmological point and diffuse sources of high energy ($30 < E < 300$ GeV) and Gamma-ray Burst Monitor (GBM) to study gamma-ray bursts. These studies led to an explosion of newly discovered Galactic and extragalactic sources.

Most of the 125 bright non-pulsar gamma ray sources detected by LAT at high latitude ($b > 10^\circ$ in the first 3 months of operation are AGNs (57 FSRQ, 42 BLLac, 6 of uncertain class and 2 radio galaxies) (39). The Galactic gamma ray sources include 13 new pulsars (40) (radio-quiet pulsars, young radio pulsars and millisecond pulsars), pulsar wind nebulae (41)(PWNe), supernova remnants, molecular clouds, X-ray binaries (42), Wolf-Rayet stars, OB associations, open clusters and globular clusters (43).

4.1. High energy gamma ray astronomy and the origin of Galactic CRs

In 1934, Baade and Zwicky proposed that supernovae are the main sources of galactic CRs which were first discovered by Hess in 1912. Today diffusive shock acceleration in the blast wave driven into the ISM by a supernova shell is the most popular model for the origin of galactic cosmic rays. Despite the general consensus and exciting recent results, the origin of these particles is still debated and an unambiguous and conclusive proof of the supernova remnant hypothesis is still missing. In particular, the recent detection of a number of supernova remnants in TeV gamma rays by HESS, MAGIC and VERITAS still does not constitute a conclusive proof that galactic cosmic rays nuclei with energies below the cosmic ray knee are accelerated mainly in supernova remnants (SNRs). In particular, it was found that it is difficult to disentangle the hadronic and leptonic contributions to the observed gamma ray emission (for an excellent review see (44)).

In some shell SNRs such as RX J1713.7-3946 and Vela Junior the non-thermal synchrotron emission exhibits a striking morphological similarity with the TeV gamma ray image. Such a correlation is naturally expected in leptonic models, where both X-rays and gamma rays are emitted by the same population of electrons via synchrotron and inverse Compton scattering, respectively. Although the correlation can be accommodated also within hadronic models if most of the gamma ray emission is through π^0 decay and the X-ray emission is the result of synchrotron emission from secondary electrons from π^\pm decay. In such a scenario the energy flux in TeV gamma rays must exceed that in X-rays since the electrons from $\pi^\pm \rightarrow \mu^\pm \rightarrow e^\pm$ decay carry less energy than the γ 's from π^0 decay, while the opposite is observed in RX J1713.7-3946. But, the assumed synchrotron radiation from secondary electrons plus positrons may not be the correct origin of the X-ray emission from RX J1713-394 (e.g. bremsstrahlung from ISM protons which enter the SN shell rest-frame

with ~ 200 keV kinetic energy). In fact, the gamma ray spectrum that was measured from this SNR by HESS up to almost 100 TeV has a knee (or an exponential cutoff) around $E \sim 5$ TeV which suggest that protons are accelerated in RX J1713.7-3946 up to the CR knee energy around 2 PeV: At 2 PeV the mean charge multiplicity (mostly pions) in pp collisions is around 50 and that of the π^0 's is about 25. Pions carry about 35% of the incident proton energy and about 1/3 of that energy is carried by π^0 's. Consequently, the typical energy of photons from the decay of π^0 produced by 2 PeV protons in pp collisions is roughly 5 TeV.

However, the safest way of proving or rejecting acceleration of CR nuclei in RX J1713.7-3946 (and in SNRs in general) is to search for neutrinos produced in the decay of charged pions (by stacking all the neutrino events from the direction of known SNRs).

4.2. High energy gamma ray emission in GRBs

During nearly 20 years of observations the Burst And Transient Source Experiment (BATSE) on board the Compton Gamma Ray Observatory (CGRO), has detected and measured light curves and spectra in the keV-MeV range of several thousands Gamma Ray Bursts (GRBs). Higher-energy observations with its EGRET instrument aboard CGRO were limited to those GRBs which happened to be in its narrower field of view. Its large calorimeter measured the light-curves and spectra of several GRBs in the 1-200 MeV energy range. Seven GRBs were detected also with the EGRET spark chamber, sensitive in the energy range 30 MeV - 10 GeV. The EGRET detections indicated that the spectrum of bright GRBs extends at least out to 1 GeV, with no evidence for a spectral cut-off (see, e.g., Dingus 2001, and references therein). However, a few GRBs, such as 940217 (45) and 941017 (46) showed evidence for a high energy component in the GRB pulses which begins significantly after the beginning of the keV- MeV pulse and has a slower temporal decay than that of the keV-MeV emission, suggesting that the high-energy emission, at least in some cases, is not a simple extension of the main component, but originates from a different emission mechanism and/or region. This has been confirmed recently by observations of high energy photons from several GRBs with the Fermi LAT (49),(50),(51), and AGILE (48). However, the flux levels of TeV gamma rays from a couple of GRBs which were inferred from ground level measurements of atmospheric showers were not confirmed by HESS with its high sensitivity array which produced upper limits much smaller than the flux levels predicted by standard fireball models where TeV photons are produced by inverse Compton scattering, decay of π^0 's from proton-gamma collisions and synchrotron radiation from UHE protons.

Not only the observed flux levels but also the spectral and temporal behaviour of the high energy emission are not those predicted by the popular fireball (FB) models of GRBs.

This is not completely surprising in view of the fact that the rich and accurate data, which have been accumulated in recent years from space-based observations with Swift and ground based observations with robotic telescopes, have already challenged the prevailing popular views on GRBs: Synchrotron radiation (SR) cannot explain simultaneously their prompt optical emission and their hard X-ray and gamma-ray emission which were well measured in some bright GRBs such as 990123 and 080319B (Figs. 8,??). The prompt hard X-ray and gamma-ray pulses cannot be explained by synchrotron radiation from internal shocks generated by collisions between conical shells. Neither can SR explain their typical energy, spectrum, spectral evolution, pulse-shape, rapid spectral softening during their fast decay phase and the established correlations between various observables. Moreover, contrary to the predictions of the FB model, the broadband afterglows of GRBs are highly chromatic at early times, the brightest GRBs do not show jet breaks, and in canonical GRBs where breaks are present, they are usually chromatic and do not satisfy the closure relations expected from FB model jet breaks. In spite of all the above, the GRB community is not so critical and many authors believe that the GRB data require only some modifications of the standard FB model in order to accommodate the observations. Other authors simply ignore the failures of the FB model and continue the interpretation of observations with the FB model hypotheses (colliding conical shells, internal and external shocks, forward and reverse shocks, continuous energy injection, refreshed shocks) and parametrize the data with freely adopted formulae (segmented power laws, exponential-to power-law components) which were never derived explicitly from any underlying physical assumptions.

In spite of the above, not all authors are so critical and they believe that the GRB data require only some modifications of the standard FB model in order to accommodate the observations. Many papers, including some presented at this Rencontre seem to ignore the failures of the FB model and continue to interpret the observations with the FB model hypotheses and parametrize the data with freely adopted formulae.

The situation of the cannonball (CB) model of GRBs is entirely different. In a series of publications, which were largely ignored by the rest of the GRB community, it was demonstrated repeatedly that the model correctly predicted the main observed properties of GRBs and reproduces successfully the diverse broad-band light-curves of both long GRBs (53) and short hard bursts (SHBs) (54). In fact since the discovery of GRBs in 1967 and the beginning of the GRB debate, the majority view on key GRB issues initially was always wrong, while a minority view turned out to be the right one, as demonstrated in Table I where the ‘correct view’ is indicated by bold letters.

In the CB model, a highly relativistic jet of plasmoids (CBs) from the central engine first encounters a cavity produced by the wind/ejecta blown by the progenitor star (SN-

GRBs) or by a companion star or an accretion disk in abinary system (SHBs) and filled up with quasi isotropic radiation (glory) emitted/scattered by by the wind/mass ejecta prior to the GRB. The prompt gamma-ray and X-ray emission is dominated by inverse Compton scattering (ICS) of this glory light. A simultaneous broad band synchrotron radiation (SR) and inverse Compton scattering of this radiation to much higher energies begin slightly after the CBs have swept in enough electrons and ionized nuclei of the ejecta/wind in front of them, isotropized them and Fermi accelerated them and the knocked-on (Bethe-Bloch) electrons and nuclei in the CBs to high energy by their turbulent magnetic fields. SR from these electrons dominates the optical radiation, while ICS of these SR photons (SSC) produces high energy photons with an energy flux density that extends beyond TeV. Production of π^0 's in collisions between the Fermi accelerated nuclei and the ambient matter in the CBs and the wind produces a power-law distribution of high energy photons which extends to much higher energies. The same mechanisms can produce also the observed high energy emission from short hard bursts (SHBs). Like for blazars, the observed flux of high energy photons from ordinary GRBs and SHBs is suppressed significantly at TeV energies by pair production in the IGM, while in the energy range covered by LAT, the absorption of photons by the extragalactic background light can be negligible.

5. High energy gamma ray astronomy, UHECRs and the extragalactic background light

Pair production in collisions of high energy photons with extragalactic background light (EBL) from the far infrared strongly modifies the flux and spectrum of high energy (0.1-100 TeV) photons from distant point and diffuse sources. Measurements of these fluxes from various bright sources such as AGNs and GRBs as function of redshift can be used to test and constrain theoretical models of star and dust formation, structure formation in the early universe, astrophysical models of HE cosmic sources and photon-photon interaction at very high energies. Photodisintegration of UHECR nuclei in their collisions with EBL photons strongly affects their composition(55). TeV gamma rays from blazars have been used extensively to test the measurements and theoretical estimates of the EBL (see (56) and Fig. 10), the strongest constraints come from the most distant blazar 3C279 at $z=0.536$, which has been detected by MAGIC (58) in TeV gamma rays. Detection of a 13 GeV photon from GRB 080916C with the Fermi LAT at redshift $z=4.35$ has also been used already to test different EBL models (52).

5.1. HE gamma rays from extragalactic sources

Despite the detection of a dozen of extragalactic blazars in TeV by HESS (57), MAGIC (58) and VERITAS (59) and ten times more in GeV photons by Fermi LAT (60),(39) and despite the multi wavelength campaigns (e.g. (61) where a few of these extragalactic sources were observed simultaneously in the radio, optical, X-ray, GeV and TeV bands, beside constraining some theoretical models, not much better understanding of how massive black holes launch their mighty jets has been achieved. This is because of the complexity of the black hole engine, the complexity of its environment, the complex time variability of the observed emission and the very many adjustable parameters and assumptions in the theoretical models. Roughly, most observations are consistent with a leptonic SSC model where synchrotron radiation from a population of Fermi accelerated electrons with a typical peak flux energy E_{SR} suffers inverse Compton scattering by the same population of electrons. The relativistic kinematics and the energy dependence of the Klein-Nishina cross section of ICS produces a second peak at $E_{SSC} \approx (m_e c^2)^2 \delta^2 / 3 E_{SR} (1+z)^2$ where δ is the Doppler factor of the Blazar's jet.

Acknowledgments

The author would like to thank all the speakers at the 44th Rencontre De Moriond on High Energy Phenomena in the Universe, the scientific organizing committee for a most interesting program, and in particular Jean Tran Thanh Van and Kim who step aside after having initiated and organized the past 44 Rencontres de Moriond in order to promote scientific collaboration, scientific exchange and spread of scientific knowledge beyond borders and ideological and racial barriers. John Belz, Marusa Bradac, Francesco Cafana, Gudlaugur Johannesson, Daniel Mazin, Aldo Morselli and Michael Schubnell are gratefully acknowledged for supplying original figures for this summary.

REFERENCES

- (1) K. Greisen, Phys. Rev. Lett. **16**,748 (1966).
- (2) G.T. Zatsepin, V.A. Kuz'min, JETP Lett. 4, 78 (1966).
- (3) D. Allard, these proceedings and references therein.
- (4) M. Takeda et al. Phys. Rev. Lett. **81**, 1163 (1998).

- (5) A. Abbasi et al, Phys. Rev. Lett. **100**, 101101 (2008).
- (6) J. Belz, these proceedings and references therein.
- (7) J. Abraham et al., Phys. Rev. Lett. **101**, 061101 (2008),
- (8) F. Schuessler, these proceedings and references therein.
- (9) J. Abraham et al., Science **318**, 939 (2007).
- (10) J. Abraham et al., Astropart. Phys. **29**, 188 (2008).
- (11) A. Mariazzi, these proceedings and references therein.
- (12) R. Knapik, these proceedings and references therein.
- (13) V. Scherini, these proceedings and references therein.
- (14) J.P. Rachen, P. L. Biermann, Astron. & Astroph., **272**, 161 (1993).
- (15) J.D. Beckenstein, Phys. Rev. D, **70** 083509 (2004).
- (16) J.R. Brownstein, J.M. & Moffat, J. W. MNRAS, **367**, 527 (2006).
- (17) M. Bradac, these proceedings, and references therein.
- (18) M. Bradac et al., Astrophys. J. **652**, 937 (2006).
- (19) M. Bradac et al., Astrophys. J. **687**, 959 (2008).
- (20) S.D. Hunter et al., Astrophys. J. **481**, 205 (1997).
- (21) W. de Boer et al., Phys. Rev. Lett. **95**, 209001 (2005) and references therein.
- (22) G. Johannesson, these proceedings and references therein.
- (23) F.W. Stecker, S.D. Hunter & D. A. Kniffen, Astropart. Phys. **29**, 25 (2008).
- (24) J. Chang et al., Nature, **452**, 362 (2008).
- (25) C. Cheng, J. L. Feng & K. T. Matchev, Phys. Rev. Lett. **89**, 211301 (2002); D. Hooper & K. Zurek, arXiv:0902.0593 (2009) and references therein.
- (26) M. Schubnell, these proceedings and references therein.
- (27) S. Dado & A. Dar, arXiv:0903.0165 (2009).

- (28) P. Sreekumar et al., *Astrophys. J.* **494**, 523 (1998).
- (29) A.R. Fazely, R.M. Gunasingha, S.V. Ter-Antonyan, arXiv:0904.2371v3 (2009)
- (30) F. Aharonian et al., arXiv:0905.0105 (2009).
- (31) A.A. Abdo et al., arXiv:0905.0025 (2009).
- (32) F. Cafana, these proceedings and references therein.
- (33) A. Morselli, these proceedings and references therein.
- (34) O. Adriani et al., *Nature* **458**, 607, 2009
- (35) I.V. Moskalenko & A.W. Strong, *Astrophys. J.* **493**, 694 (1998).
- (36) N. Kawanaka, these proceedings and references therein.
- (37) T. Piran, N. Shaviv & E. Nakar, these proceedings.
- (38) A. Dar & A. De Rújula, *Phys. Rep.* **466**, 179, (2008).
- (39) B. Lott, these proceedings and references therein.
- (40) F. Giordano, these proceedings and references therein.
- (41) M.H. Grondin, these proceedings and references therein.
- (42) A. Hill, these proceedings and references therein.
- (43) D.A. Smith, these proceedings and references therein.
- (44) S. Gabici arXiv:0811.0836 (2008).
- (45) K. Hurley et al., *Nature* **372**, 652 (1994).
- (46) M.M. Gonzalez et al., *Nature* **424**, 749 (2003).
- (47) B.L. Dingus,, in *High Energy Gamma Ray Astronomy*, AIP Conf. Proc. **558**, 383 (2001).
- (48) A. Giuliani et al., *Aston. & Astrophys.* **491**, L25 (2008).
- (49) L. Baldini, these proceedings and references therein.
- (50) V. Pelassa, these proceedings and references therein.
- (51) J. Granot, these proceedings and references therein.

- (52) A.B. Abdo et al., *Science* **323**, 1688 (2009).
- (53) S. Dado, A. Dar & A. De Rújula *Astrophys. J.* **696**, 994 (2009).
- (54) S. Dado, A. Dar & A. De Rújula, *Astrophys. J.* **693** 311 (2009).
- (55) J.L. Puget et al., *Astrophys. J.* **205** 638, 1976.
- (56) D. Mazin, these proceedings and references therein.
- (57) L. Gerard, these proceedings and references therein.
- (58) B. De Lotto, these proceedings and references therein.
- (59) W. Benbow, these proceedings and references
- (60) J. Ballet, these proceedings and references therein.
- (61) D. Sanchez, these proceedings and references therein
- (62) M.S. Briggs et al., *ApJ*, **524**, 82 (1999)
- (63) S. Dado & A. Dar, arXiv arXiv:0812.3340 (2008)
- (64) C. Akerlof et al. *Nature*, **398**, 400 (1999)
- (65) J.L. Racusin, et al. *Nature*, **455**, 183 (2008)
- (66) S. Dado, A. Dar & A. De Rújula *Astrophys. J.* **680**, 517 (2008).
- (67) S. Dado, A. Dar & A. De Rújula *Astrophys. J.* **681**, 1408 (2008).

Table 1: Evolution of the GRB debate

Issue	Majority View	Minority View	Observational Proof (Year)
Origin	Man Made	Nature Made	Vela Satellites (1967-1973)
Location	Solar System Galactic Disk Galactic Halo	More Distant Cosmological Distant Galaxies	Vela Satellites (1967-1973) CGRO (1992) BeppoSAX+HST+GBTs (1997)
Event	n^*-n^* Merger	SN Explosion	BeppoSAX+HST+GBTs (1998-2003)
Source	Relativistic Fireball Collimated Fireball/ Conical Jet	Relativistic Jet Relativistic Jet	CGRO, BeppoSAX (1992-1999) Swift+GBTs (2004-2009)
Prompt Radiation: keV-MeV "Prompt Optical" Afterglow: Chromaticity Plateau phase Jet Break when: "Missing Break"	Synchrotron Reverse Shock Achromatic Reenergization $1/\Gamma_{jet} \approx \theta_{jet}$ Very Late Break	Inverse Compton Synchrotron Chromatic Slow Deceleration $\Delta M \approx M_0(\text{jet})$ Very Early Break	BeppoSAX, Swift (1999-2009) Robotic Telescopes (1999-2009) Swift+Robotics+GBTs (2004-2009) Swift+GBTs 2004-2009 Swift+GBTs (2004-2009) Swift+GBTs (2004-2009)
To be determined ?			Observational Proof by ?
Jet Geometry Jet Composition Beamed E_γ	Conical Shells e^+e^- plasma $\sim 10^{51}$ erg	Cannonballs Ordinary Matter $\sim 10^{48}$ erg	Swift,Fermi,HST,GBTs Swift,Fermi, HST,GBTs Swift,Fermi,HST,GBTs
Source	Hypernova (Rare SNIb/c)	Normal SNIb/c Most SNIb/c	Integral, Swift, Fermi, HST,GBTs Integral, Swift,Fermi,HST,GBTs
Radiations: keV-MeV γ 's HE γ 's HE Neutrinos	SSC of ? ? Detectable by	ICS of Glory Light SSC + $pp \rightarrow \pi^0$ Not Detectable by:	Swift,Fermi,GBTs LAT,HESS,MAGIC,VERITAS,PAO ICECUBE,ANTARES,PAO
Remnant	BH, Magnetar	n^* , BH	Swift,Fermi,HST,GBTs
XRFs	Not GRBs	Far off-axis GRBs	Swift,Fermi,HST,GBTs

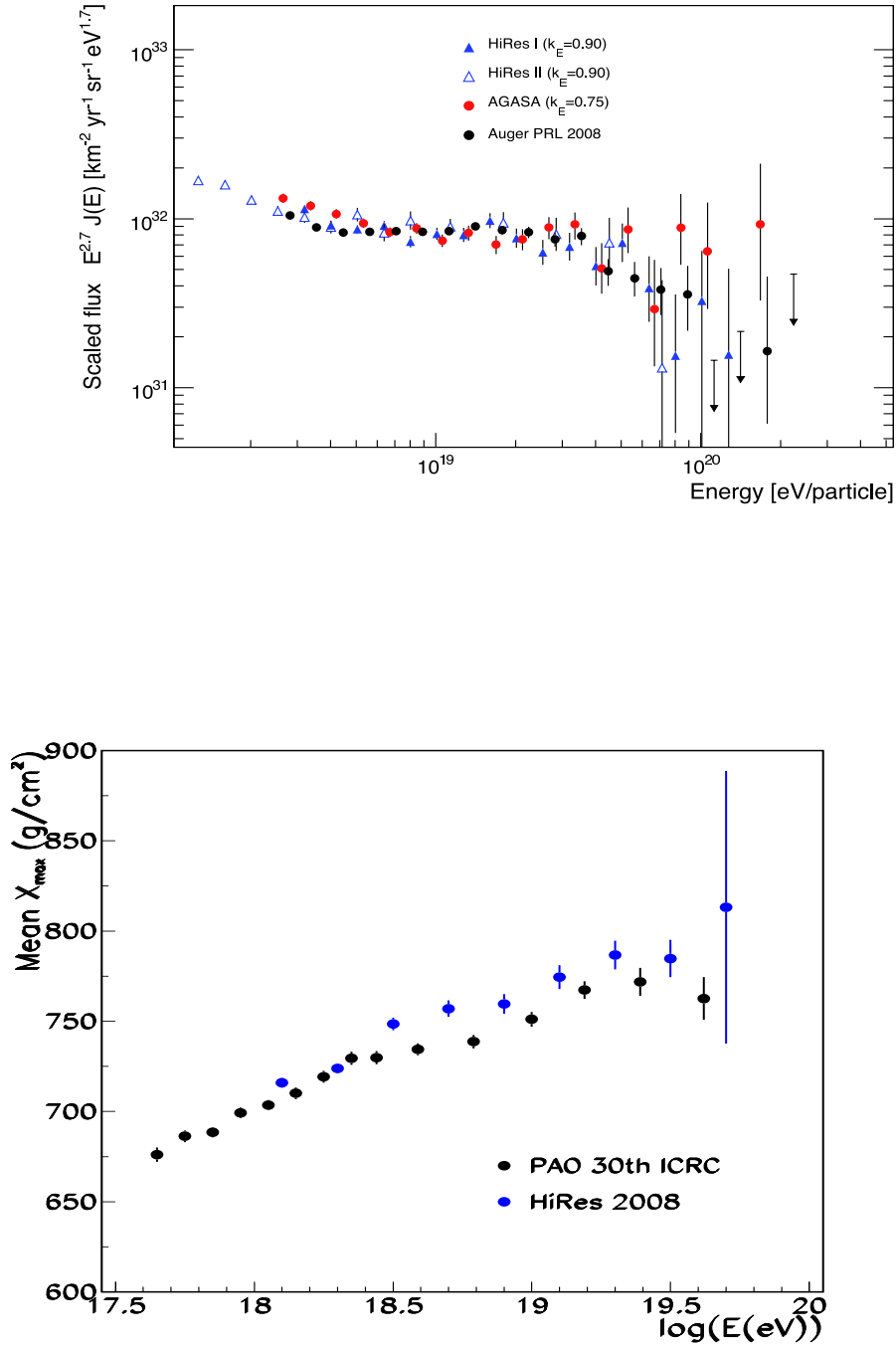


Fig. 1.— **Top (a):** Comparison between the spectra of UHECRs multiplied by $E^{2.69}$ measured by PAO, HiRes (with energy rescaled by a factor 0.9) and AGASA (with energy rescaled by a factor 0.7). The PAO and HiRes data are consistent and show the expected GZK suppression above 4×10^{19} eV. **(Bottom (b):** Comparison between the mean depth of shower maximum of UHECRs as measured by HiRes and by PAO.

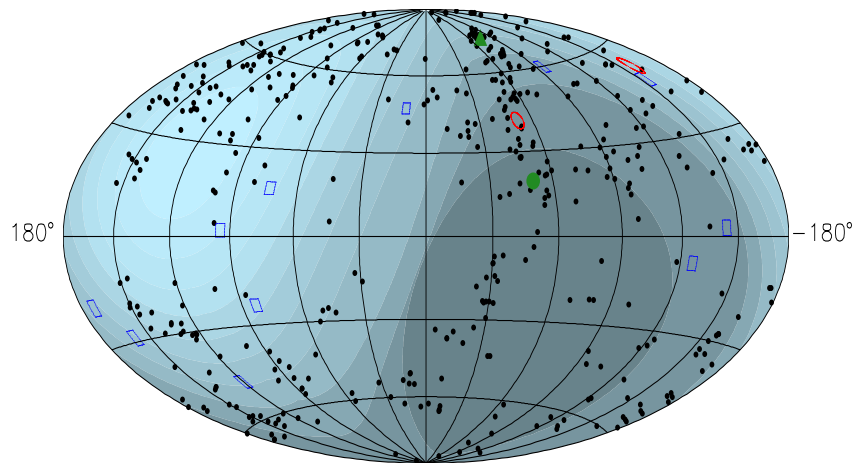
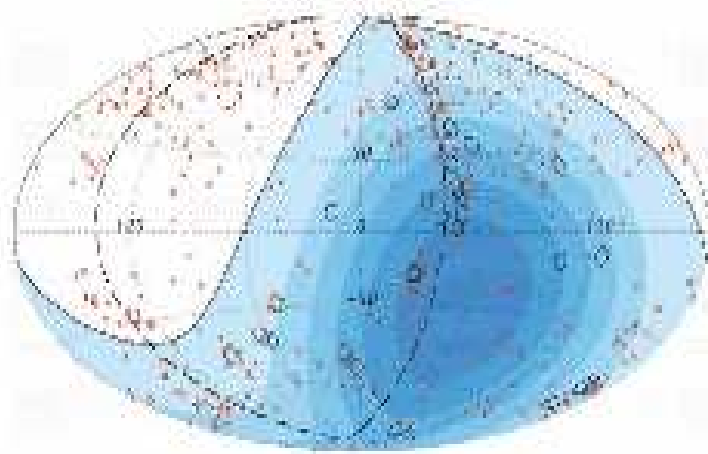


Fig. 2.— **Top (a):** The arrival directions of UHECRs with energy above 57 EeV, measured by PAO and plotted as circles with an angular radius of 3.2° centered on their arrival direction on a sky map (Galactic coordinates) of AGNs within 71 Mpc from Earth. Colors indicate equal exposure. **Bottom (b):** The arrival directions of UHECRs with energy above 57 EeV, measured by PAO and plotted as circles with an angular radius of 3.2° centered on their arrival direction on a sky map (Galactic coordinates) of AGNs within 71 Mpc from Earth. Colors indicate equal exposure.



Fig. 3.— Composite images of the bullet cluster 1E 0657-56 (**Top (a)**) and the cluster MACS J0025 (**Bottom (b)**). Both clusters were formed by a collision of two galaxy clusters. The major components of the clusters are shown in different colors., The galaxies whose stars makes them visible in optical light are shown in orange and white, the ionized gas in the clusters which is visible in X-rays is shown in pink and the putative dark matter, which dominates their gravitational potential and is inferred through gravitational lensing of background galaxies, is shown in blue. After the collision, most of the matter in the clusters (in blue) is well separated from most of the normal matter (the gas in pink) and moves ahead of it. This separation provides direct evidence that most of the matter in the clusters is dark matter which cannot be represented by modified gravity of the cluster gas which contains most of the baryons in clusters. Credits 1E0657-56: X-ray NASA/CXC/CfA Optical: NASA/STScI; Magellan/U.Arizona; Clowe et al. (2006); Bradac et al. (2006) MACS J0025 4-1222: X-ray(NASA/CXC/Stanford/S Allen): Optical/ Lens-

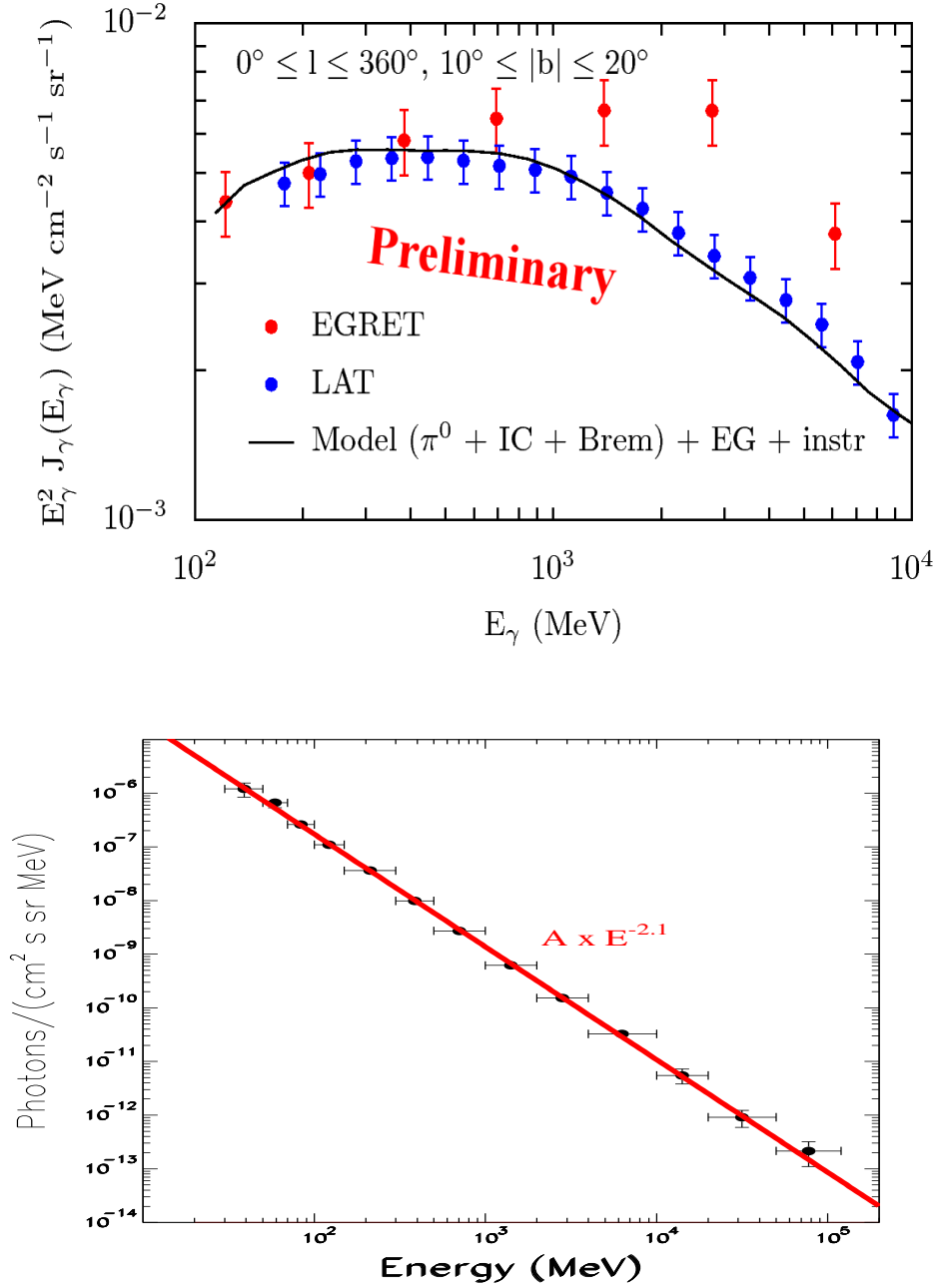


Fig. 4.— **Top (a):** Comparison between the spectra of the diffuse gamma ray background radiation at intermediate latitude which were measured by EGRET (20) and by LAT (22). The LAT data do not confirm the existence of the EGRET GeV excess and can be fitted by the standard model of Galactic cosmic ray electrons and nuclei with densities normalized to their respective locally observed densities. **Bottom (b):** The spectrum of the extragalactic gamma ray background radiation (GBR) which was measured by EGRET (28) and is well represented by a single power law, $dn/dE \propto E^{-2.1 \pm 0.03}$. No dark matter annihilation/decay fingerprints are evident in the EGRET extragalactic GBR.

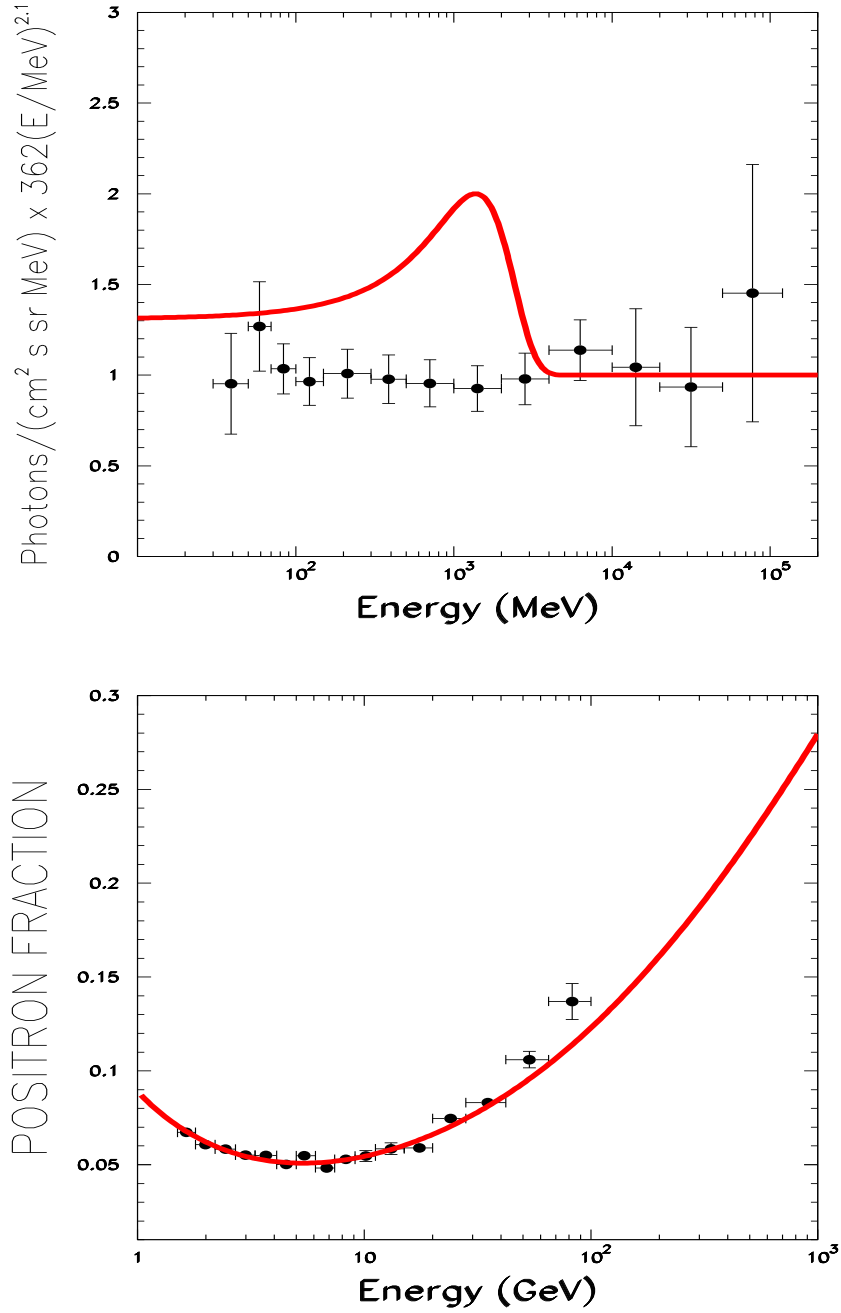


Fig. 5.— **Top (a)**: Comparison between the spectrum of the extragalactic GBR measured by EGRET (28) and a GBR spectrum which is produced by ICS of MBR photons in external galaxies by a universal power-law spectrum of high energy CR electrons, $dn_e/dE \propto E^{-3.2}$, plus a universal excess such as that measured by ATIC (24) between 300-800 GeV (27). Both spectra were divided by the best fitted power-law to the EGRET GBR spectrum. **Bottom (b)**: Comparison between the positron fraction measured with PAMELA (32),(33),(34) and that expected from secondary production of electrons and positrons in the CR sources and in the ISM (27).

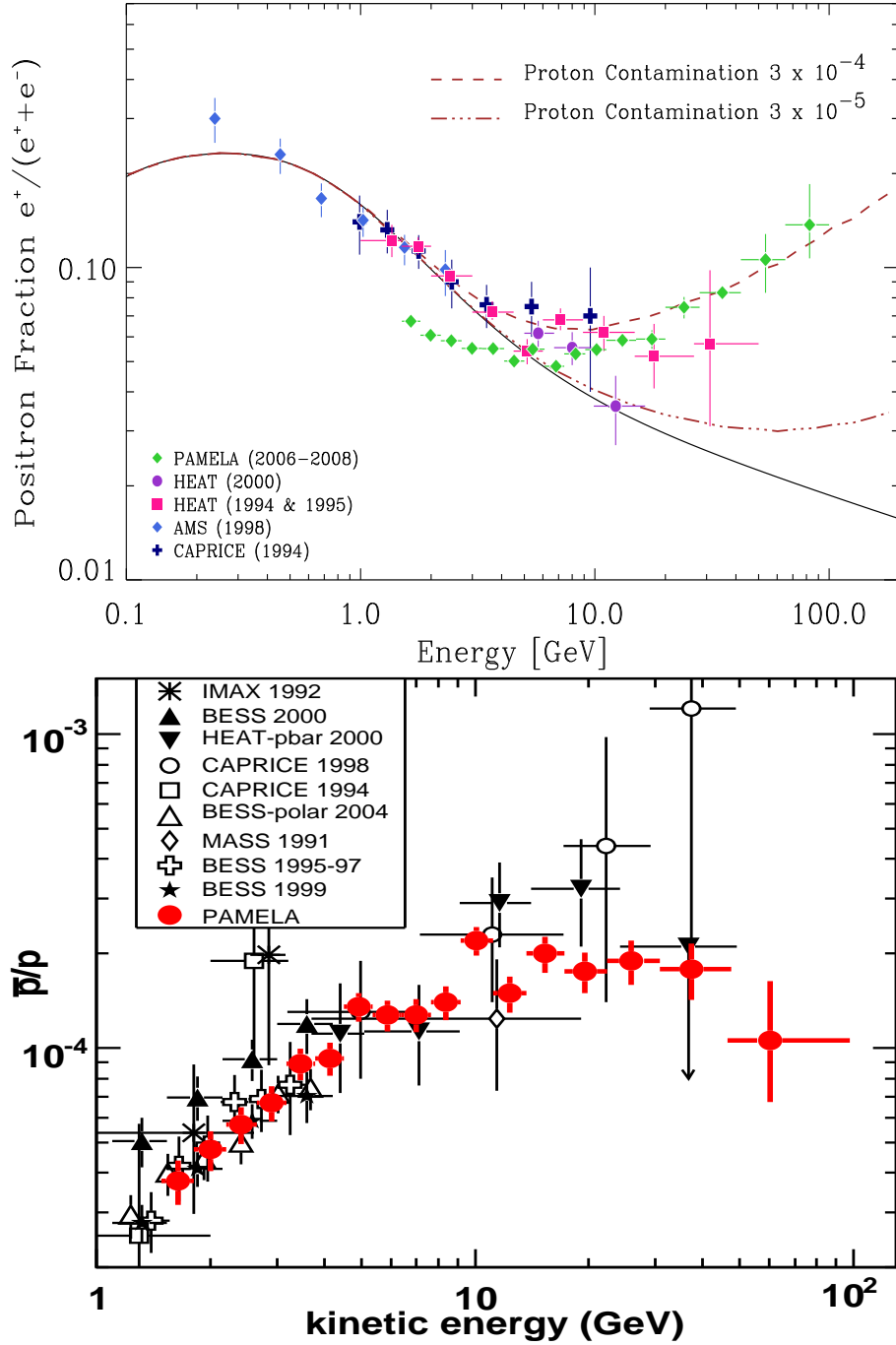


Fig. 6.— **Top (a):** Recent measurements of the positron fraction overlaid with a the standard leaky box model prediction (35) of secondary production of cosmic-ray positrons in the ISM and the same prediction including residual proton contamination (26). Below 5 GeV solar modulation affects the particle intensities observed near Earth and may explain the discrepancy between the PAMELA data and older measurements, obtained at distinctively different solar epochs. In the region between 5 and 50 GeV measurements by PAMELA are consistent with previous data from the HEAT experiment. **Bottom (b):** Comparison between the antiproton to proton ratio in Galactic cosmic rays as function of energy as measured by PAMELA and by previous experiments. The results of PAMELA cannot distinguish yet between a ratio decreasing with energy as expected from secondary production of antiprotons in the ISM, and roughly a constant ratio expected from secondary production

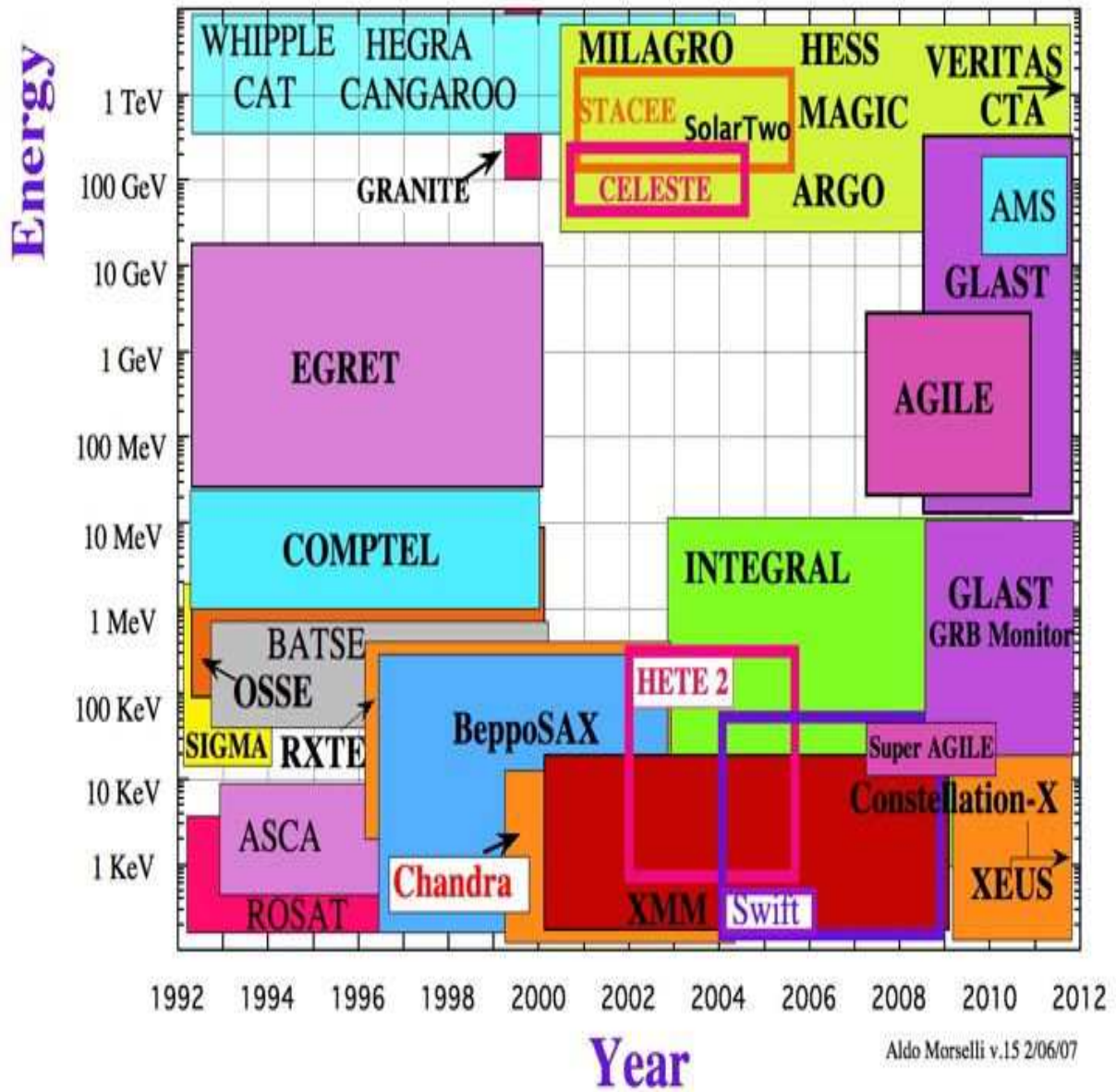


Fig. 7.— The increasing energy range and sky coverage in the past 20 years by water and air-shower Cherenkov telescopes and by gamma ray telescopes aboard satellites.

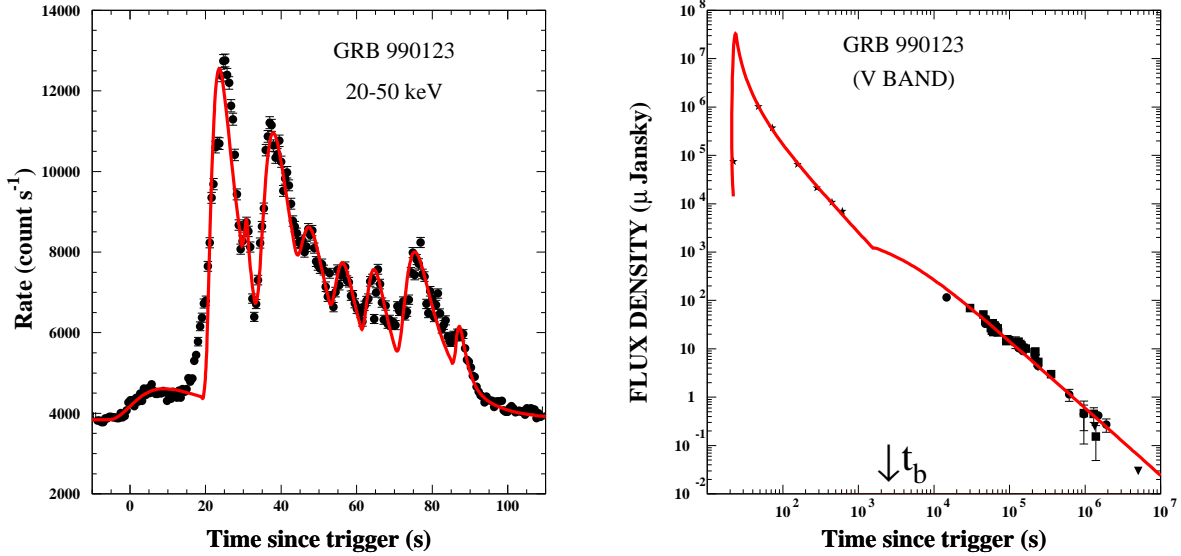


Fig. 8.— **Top (a):** Comparison between the 20-50 keV BATSE lightcurve of GRB990123 (62) and its CB model description (63). The sub-pulse superimposed on the decaying tail of the three major pulses may be due to the crossing of the 3 leading CBs through two successive wind layers (2 separate pre-supernova mass ejections by the progenitor star) rather than by 3 additional CBs. **Bottom (b):** The entire *V* band lightcurve of GRB 990123 and its CB model description as a synchrotron emission from the collision of the jet of CBs with a wind (with a density profile $n \propto 1/(r-r_0)^2$ for $r > r_0$) overtaken by a constant ISM density around an observer time $t=1000$ s. The ‘prompt’ (early-time) *V* band lightcurve was measured with ROTSE (64) which did not resolve it into individual peaks. It shows a time lag of several seconds of the prompt optical emission relative to the prompt keV-MeV emission.

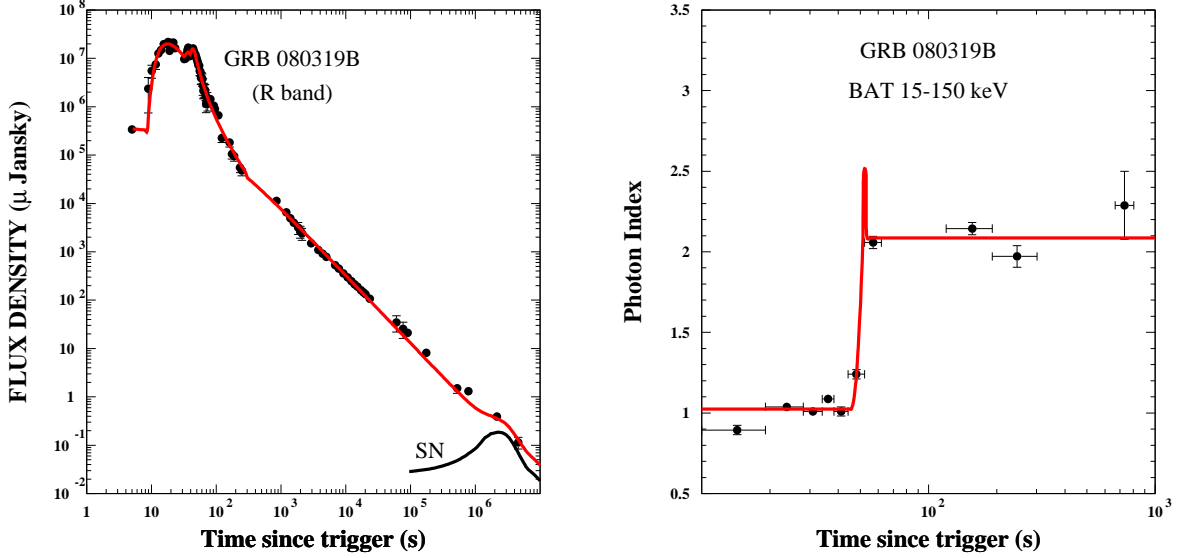


Fig. 9.— **Top (a)**: The entire *R*-band (and *V* band renormalized to the *R* band) lightcurve of GRB080319 (65) and its CB model description as synchrotron radiation from an initially expanding 3 leading CBs which merged into a single CB by the time they met the constant density ISM at the end of the prompt ICS emission of gamma-rays and hard X-rays around 300 s (observer time). Note that the prompt optical emission began about 10 seconds after the beginning of the keV-MeV emission. Shown also is the contribution to the *R*-band afterglow from SN akin to SN1998bw displaced to the GRB site. **Bottom (b)**: The mean photon spectral index in the 15-150 keV band as measured with the Swift broad alert telescope (BAT) (65) and its CB model prediction. In the CB model, the prompt emission is dominated by ICS of thin bremsstrahlung with a typical $\Gamma \approx 1$, which increases rapidly during the fast decay phase of the prompt emission and becomes ≈ 2.1 the typical value predicted by the CB model as soon as SR dominates the X-ray emission (67).

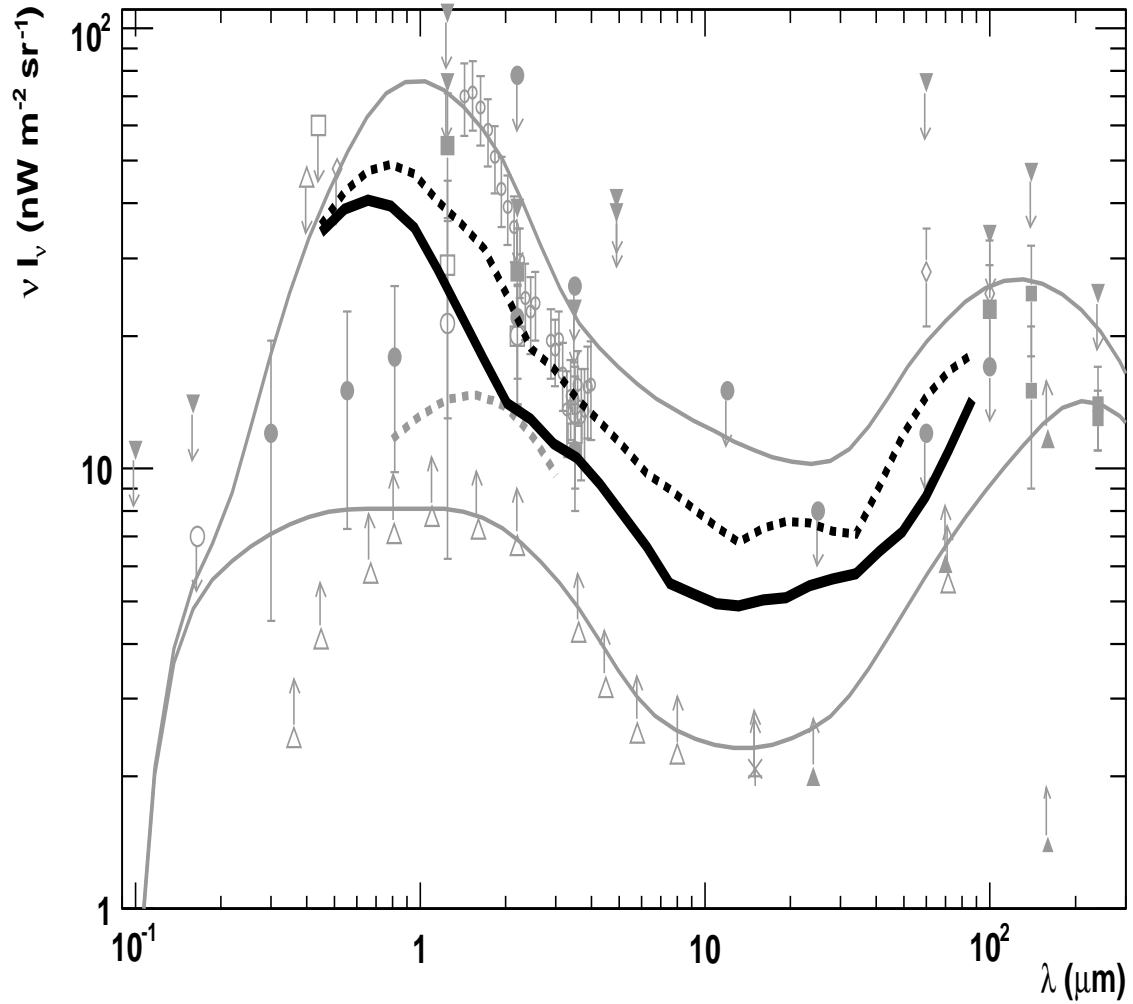


Fig. 10.— Limits and estimates of the spectrum of the extragalactic background light (EBL) as extracted from different measurements and theoretical models prior to the detection of the blazar 3C279 by MAGIC in TeV gamma rays (56).